

## NUMERICAL SIMULATION OF III-V SOLAR CELLS USING D-AMPS

M. Barrera<sup>1,2</sup>, F. Rubinelli<sup>3</sup>, J. Plá<sup>1,2</sup>, I. Rey-Stolle<sup>4</sup>

<sup>1</sup>Gerencia Investigación y Aplicaciones - Centro Atómico Constituyentes - CNEA

<sup>2</sup>Consejo Nacional de Investigaciones Científicas y Técnicas (CONICET)

Av. General Paz 1499 - 1650 San Martín - Argentina

Tel. +54-11 6772-7168, Fax +54-11 6772-7121, [www.tandar.cnea.gov.ar](http://www.tandar.cnea.gov.ar),

<sup>3</sup>INTEC-CONICET, Güemes 3450, 3000 Santa Fe – Argentina

<sup>4</sup>Instituto de Energía Solar – Universidad Politécnica de Madrid

Av.. Complutense 30; 28040 Madrid -Spain

Corresponding author: M. Barrera, e-mail: barrera@tandar.cnea.gov.ar

**ABSTRACT:** Numerical simulation of devices plays a crucial role in their design, performance prediction, and comprehension of the fundamental phenomena ruling their operation. Here, we present results obtained using the code D-AMPS-1D, that was conveniently modified to consider the particularities of III-V solar cell devices. This work, that is a continuation of a previous paper regarding solar cells for space applications, is focused on solar cells structures than find application for terrestrial use under concentrated solar illumination. The devices were fabricated at the Solar Energy Institute of the Technical University of Madrid (UPM). The first simulations results on InGaP cells are presented. The influence of band offsets and band bending at the window-emitter interface on the quantum efficiency was studied. A remarkable match of the experimental quantum efficiency was obtained. Finally, numerical simulation of single junction n-p InGaP-Ge solar cells was performed.

**Keywords:** III-V semiconductors, simulation, solar cell, concentration

### 1 INTRODUCTION

The higher efficiencies and radiation resistance of III-V solar cells have made them attractive both for space and terrestrial applications [1-4]. Given the importance acquired by PV devices based on III-V materials, a scientific collaboration from the Solar Energy Group (GES) of the National Atomic Energy Commission (CNEA, Argentina) and the Solar Energy Institute of the Technical University of Madrid (UPM, Spain) was initiated. The purpose of this cooperation is to generate a more detailed knowledge of these devices by combining the complementary experiences of both groups.

In this paper, research activities performed on InGaP and Ge solar cells, particularly in the topics of simulation and characterization, are reviewed.

This work is a continuation of previous contributions on simulation on III-V devices already published [5,6], where further details about the numerical simulations performed can be found.

### 2 NUMERICAL SIMULATION

The electrical transport and the optical behaviour of the solar cells discussed in this work were studied with the simulation code D-AMPS-1D [7,8]. This software is an updated version of the one-dimensional (1D) simulation program AMPS (Analysis of Microelectronic and Photonic Devices) that was developed at The Pennsylvania State University, University Park, USA, during the years 1988–1993 [9].

The code evaluates the external device characteristic curves such as the current density–voltage ( $J$ – $V$ ) under dark and under illumination, the quantum efficiency, the reflectivity, and internal quantities such as the electric field, the free and trapped carrier concentrations, the electron and hole currents, the recombination and generation rates, etc.

The solar cells analysed were InGaP and Ge solar cells, both of them fabricated at UPM.

The first device simulated was a single junction n-p InGaP solar cell with a structure identical to the top cell of a high efficiency high-concentrator InGaP/GaAs dual-junction solar cell [4] (details about the structure are summarised in Table I). Accordingly, their manufacturing process is identical to that used for dual-junction concentrator devices that can be found elsewhere [4], and it is based on the metal organic vapor phase epitaxy (MOVPE) technique. The active area of the solar cells is a square of 1mm of side, endowed with an inverted square grid having 8 evenly spaced fingers 3  $\mu\text{m}$  wide each and surrounded by a busbar 100  $\mu\text{m}$  wide.

The main parameters used in the simulations are summarised in Table I. The coefficient for radiative direct recombination was set to  $7.2 \times 10^{-10} \text{ cm}^3 \text{ s}^{-1}$  for GaAs [10] and to  $1 \times 10^{-10} \text{ cm}^3 \text{ s}^{-1}$  for InGaP [11]. The dependence of the mobility with respect to the doping level was taken into account in each device layer following the model used by Ghannam *et al.* [12]. The band gap of InGaP was determined experimentally and it was found to be in agreement with the values reported in the literature for partially ordered InGaP [13-15]. Band offsets between AlInP and InGaP were taken as type 1 [16] although, in detailed simulations, the dependence of our results for different offsets was studied. In all cases the illumination source was the standard AM0 and AM1.5G, spectra taken from ASTM standards [17], since these were the spectra available at the solar simulators.

The cells lacked of an antireflective coating (ARC), a non-passivated surface was considered ( $S_f = 1 \times 10^6 \text{ cm/s}$ ), as well as some band bending at the front surface.

**Table I:** Main parameters used in the numerical simulations of the InGaP solar cell.

	window	emitter	base	BSF	buffer	substrate
Material	AlInP	InGaP	InGaP	AlGaInP	GaAs	GaAs
$E_g$ (eV)	2.36	1.82	1.82	2.13	1.424	1.424
Thickness (nm)	25 / 30	180	600	70 / 40	1150	250000
$N_d$ (cm <sup>-3</sup> )	$5.10^{17}$	$5.10^{17} / 1.10^{18}$	0	0	0	0
$N_a$ (cm <sup>-3</sup> )	0	0	$1.10^{17} / 9.10^{16}$	$5.10^{17}$	$1.10^{18}$	$1.10^{17}$
Radiative recombination rate coefficient (cm <sup>3</sup> /s)	-	$1 \times 10^{-10}$	$1 \times 10^{-10}$	$1 \times 10^{-10}$	$7.2 \times 10^{-10}$	$7.2 \times 10^{-10}$
Electron mobility (cm <sup>2</sup> /V.s)	832	895	1140	895	2834	6647
Hole mobility (cm <sup>2</sup> /V.s)	40	40	40	40	154	345

Nowadays, Ge solar cells have become important because they can be used both in homojunction and multijunction devices. An example of the first scenario is the case of devices for TPV (Thermophotovoltaics) applications [18, 19] and an example of the second are triple junction InGaP-GaAs-Ge cells for space or terrestrial applications.

The second device simulated was an InGaP-Ge solar cell. The main parameters used in the simulations are listed in Table II. The InGaP material parameters were extracted from the same references used to simulate the InGaP cell. The Ge mobility was extracted from reference [20]

**Table II:** Main parameters used in the numerical simulations of the Ge cell.

	buffer	emitter	base
Material	InGaP	Ge	Ge
$E_g$ (eV)	1.82	0.664	0.664
Thickness (nm)	980	180	180000
$N_D$ (cm <sup>-3</sup> )	$3 \times 10^{18}$	$8.5 \times 10^{18}$	-
$N_A$ (cm <sup>-3</sup> )	-	-	$1.5 \times 10^{17}$
Electron mobility (cm <sup>2</sup> /V.s)	803	1000	2600
Hole mobility (cm <sup>2</sup> /V.s)	40	200	700
Radiative recombination rate coefficient (cm <sup>3</sup> /s)	$1 \times 10^{-10}$	-	-

The emitter of InGaP-Ge solar cell was prepared by diffusion of phosphorus and the buffer was grown by MOVPE technique. The active area of the solar cells is a circle of about 1.53mm of diameter.

In the numerical simulations was taken into account that Ge solar cells, with n-p (or p-n) junction, can be prepared by two methods: dopant diffusion [19, 21] or epitaxial growth [22, 23], in both cases starting from n-type or p-type substrate. Thus, a comparison of the simulated electrical parameters of each case was performed.

### 3 RESULTS

#### 3.1 InGaP solar cell

Figure 1 shows the experimental and the simulated external quantum efficiencies (EQE) of two n-p InGaP solar cells. As can be seen in 1a and 1b, the fitting of the experimental curve is quite good. The fit in the short wavelength region can be improved adjusting the band offsets at the window - emitter interface ( $\Delta E_c$ , as shown in Figure 2). Thereby, several values for  $\Delta E_c$  have been considered in order to evaluate the deviations of our predictions with respect to the EQE experimental curve (Figure 3). The calculated electrical parameters are presented in Table III.

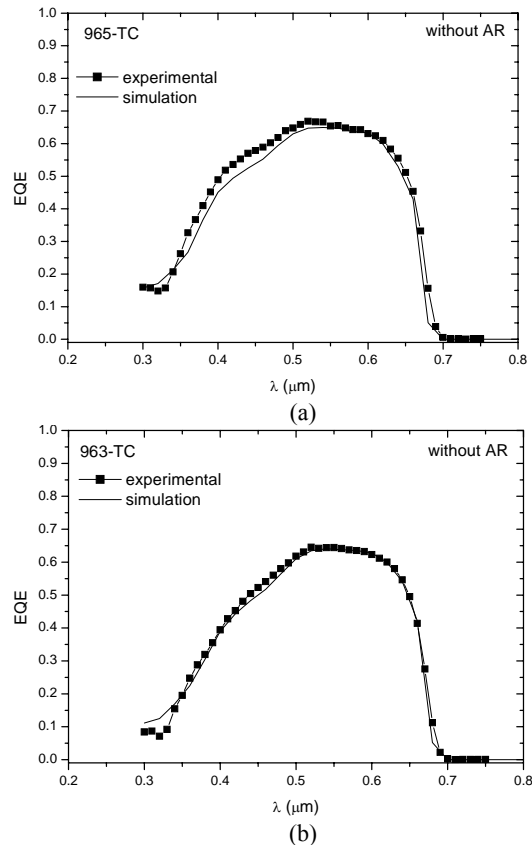


**Figure 1:** External quantum efficiency of InGaP solar cells. The experimental curve was measured at UPM. The two structures differ basically in the window and BSF thicknesses as specified in Table I.

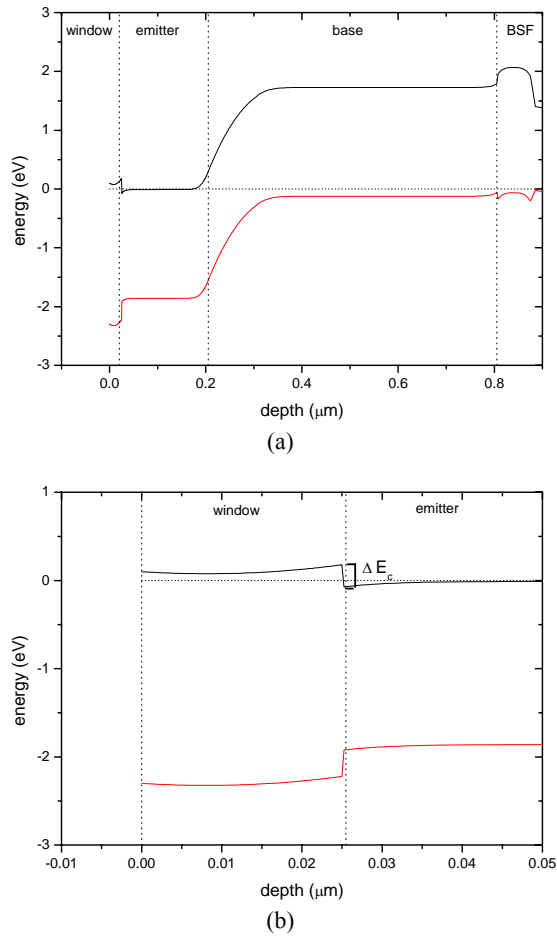


**Figure 2:** (a) Energy band diagram calculated for the InGaP cell at thermodynamic equilibrium. (b) Enlarged view showing details of the conduction band offset  $\Delta E_c$  at the window – emitter interface.

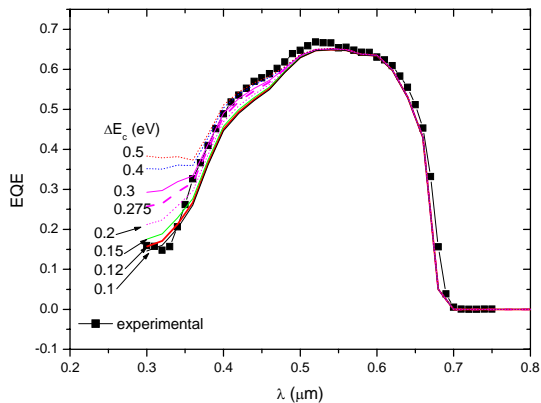


**Figure 3:** External Quantum Efficiency calculated for different values of  $\Delta E_c$ .

**Table III:** Electrical parameters calculated for the homojunction InGaP solar cells.

	$V_{oc}$ (V)	$J_{sc}$ (mA/cm <sup>2</sup> )	FF	$\eta$ (%)
965-TC				
AM0	1.32	13.07	0.826	10.40
AM1.5G	1.30	11.25	0.832	12.25
963-TC				
AM0	1.31	12.58	0.835	10.09
AM1.5G	1.30	10.98	0.837	11.92

### 3.2 Germanium solar cell

As mentioned before, the emitter of Ge homojunctions can be prepared by two methods, diffusion or epitaxial growth. The results show small differences in the electrical parameters when a gaussian or an abrupt change in the concentration of the emitter doping is considered.

Incidentally, the Ge devices were electrically characterised in the GES. The I-V curve was measured with a commercial solar simulator with 1kW Xe lamp, a customised optical filter for a better matching of the AM1.5G spectrum, and a data acquisition system. Irradiance was set with a c-Si reference cell previously calibrated. Then they were corrected according to the short circuit current measured under the Sun, where global irradiance was monitored using a thermopile type radiometer. Finally, electrical parameters were extracted from the corrected I-V curves.

The experimental and the simulated results are presented in Table IV.

**Table IV:** Light J-V parameters calculated for the Ge solar cell (AM1.5G).

	$V_{oc}$ (mV)	$I_{sc}$ (mA)	FF	$\eta$ (%)
733-BC				
experimental	230	25.00	0.644	5.7
simulation (diffused junction)	220	25.74	0.653	5.6
simulation (abrupt junction)	220	25.73	0.652	5.6

It is important to note that when a high density of defects in the buffer ( $N_d=1 \times 10^{17} \text{cm}^{-3}$ ) is considered, a better fitting for the EQE curve at low wavelengths is achieved. In this particular case, the short circuit current became  $J_{sc}=25.03 \text{mA/cm}^2$  that better approximates the experimental value. This could mean that there is a high density of defects in the material or at the InGaP-Ge interface, reaching the junction fewer electron-hole pairs generated in the InGaP.

Figure 4 shows the generation (G) and recombination rates (R) for the different device layers. The region of the substrate where  $R=G$ , about  $67 \mu\text{m}$  from the surface, is a dead zone in terms of collection of photocarriers that does not contribute to the current  $J_{sc}$ , i.e., it just plays the role of mechanical support.

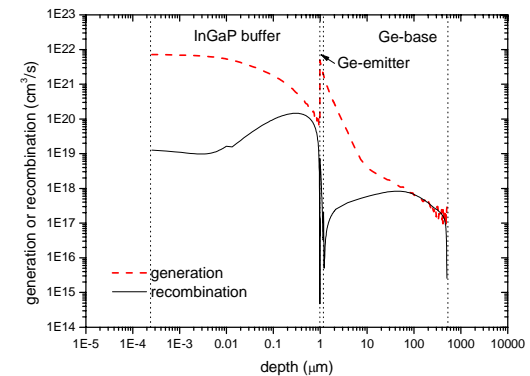


**Figure 4:** Generation and recombination rates versus depth. The front surface is not passivated ( $S_f=1 \times 10^6 \text{cm}^{-1}$ ).

#### 4 SUMMARY

New results on III-V and Ge solar cells simulation using D-AMPS-1D are presented. The main electrical and optical parameters were taken from literature and the simulated structures correspond to real devices. Particularly, in InGaP cells without ARC, the characteristics of the EQE at short wavelengths were successfully interpreted in terms of the band offset alignment at the window-emitter interface. These results demonstrate the capabilities of the D-AMPS-1D code to provide valuable insight into the performance of III-V solar cells. On the other hand, an InGaP-Ge homojunction was simulated. A comparison of the electrical parameters obtained by numerical simulation of diffused emitter and abrupt junction was made. The results show practically no differences if an average concentrated in the abrupt case is considered. Finally, the onset of the “dead zone” in the device was observed.

#### 5 ACKNOWLEDGEMENTS

This work was funded by CNEA, CONAE, and the subsidies PIP2009-2011 N° 02318 (CONICET) and PICT2007 N° 01143 (ANPCyT).

#### 6 REFERENCES

1. A.W. Bett, F. Dimroth, W. Guter, R. Hoheisel, E. Oliva, S.P. Philipps, J. Schöne, Highest efficiency multi-junction solar cell for terrestrial and space applications, Proceedings of the 24<sup>th</sup> European Photovoltaic Solar Energy Conference, (2009) 1.
2. M. Alurralde, M. Barrera, C.G. Bolzi, C.J. Bruno, P. Cabot, E. Carella, J. Di Santo, J.C. Durán, J. Fernández Vázquez, A. Filevich, E.M. Godfrin, V. Goldbeck, L. González, A. Iglesias, M.G. Martínez Bogado, E. Mezzabolta, A. Moglioni, S. Muñoz, C. Nigri, S.L. Nigro, J. Plá, I. Prario, M.C. Raffo Calderón, D. Raggio, C. Rinaldi, S.E. Rodríguez, H. Socolovsky, M.J.L. Tamasi, A. Vertanessian, Flight model for the Aurius/SAC-D satellite mission, Proceedings of the 24<sup>th</sup> European Photovoltaic Solar Energy Conference, (2009) 695.
3. M. Casale, R. Campesato, G. Gabetta, G. Gori, C. Flores, M. Kagan, V. Semenov, V. Ivanov, Triple junction solar cells and solar panels for the new generation of Russian spacecraft, Proceedings of the 24<sup>th</sup> European Photovoltaic Solar Energy Conference, (2009) 101.
4. I. García, I. Rey-Stolle, B. Galiana, and C. Algora, A 32.6% efficient lattice-matched dual-junction solar cell working at 1000 suns, Applied Physics Letters **94** (2009) 053509.
5. J. Plá, M. Barrera, F. Rubinelli, Influence of the InGaP window layer on the optical and electrical performance of GaAs solar cells, Semiconductor Science and Technology, **22**, (2007)1122.
6. M. Barrera, J. García, H. Socolovsky, F. Rubinelli, E. Godfrin, J. Plá, Activities on simulation and characterization of multijunction solar cells for space applications in Argentina, Proceedings of the 23<sup>rd</sup> European Photovoltaic Solar Energy Conference, (2008) 781.
7. F.A. Rubinelli, J.K. Rath, R.E.I. Schropp, Microcrystalline n-i-p tunnel junction in a-Si:H/a-SiH tandem cells, Journal of Applied Physics **89** (2001) 4010.
8. M. Vukadinovic, F. Smole, M. Topic, R.E.I. Schropp, F.A. Rubinelli; Transport in tunnelling recombination junctions, a combined computer simulation study, Journal of Applied Physics **96** (2004) 7289.
9. P.J. McElheny, J.K. Arch, H.S. Lin, S.J. Fonash, Range of validity of the surface-photovoltage diffusion length measurement: a computer simulation, Journal of Applied Physics **64** (1988) 1254.
10. M. Levinstein, S. Rumyantsev, M. Shur, Handbook Series on Semiconductor Parameters Vol 1 (1996), World Scientific.
11. M. Levinstein, S. Rumyantsev, M. Shur, Handbook Series on Semiconductor Parameters Vol 2 (1999), World Scientific.
12. M. Ghannam, J. Poortmans, J. Nijs, R. Mertens, Theoretical study of the impact of bulk and interface recombination on the performance of GaInP/GaAs/Ge triple junction tandem solar cells, Proceedings of the 3<sup>rd</sup> World Conference on Photovoltaic Energy Conversion, (2003) 666.
13. W.E. McMahon, S. Kurtz, K. Emery, M.S. Young, Criteria for the design of GaInP/GaAs/Ge triple-junction cells to optimize their performance outdoors, Proceedings of the 29<sup>th</sup> IEEE Photovoltaic Specialists Conference, (2002) 93.
14. D.N. Keener, D.C. Marvin, D.J. Brinker, H.b. Curtis, P.M. Price, Progress toward technology transition of GaInP<sub>2</sub>/GaAs/Ge multijunction solar cells, Proceedings 26<sup>th</sup> IEEE Photovoltaic Specialists Conference, (1997) 787.
15. J.M. Olson, D.J. Friedman, S. Kurtz, High Efficiency III-V Multijunction Solar Cells, Handbook of Photovoltaic Science and Engineering, ed. A. Luque and S. Hegedus (2003), Wiley.
16. E.F. Schubert, Physical Foundations of Solid-State Devices, (2005) <http://www.rpi.edu/~schubert/>
17. Available in <http://rredc.nrel.gov/solar/spectra/>
18. B. Galiana, I. Rey-Stolle, I. Garcia, A. Datas, C. Algora, MOVPE growth on Ge substrates for thermophotovoltaic cell applications, Proceedings of the EW-MOVPE XII, (2007) D6.
19. N.E. Posthuma, J. van der Heide, G. Flamand, J. Poortmans, Emitter formation and contact realization by diffusion for germanium photovoltaic devices, IEEE Transactions on Electron Devices **54** (2007) 1210.
20. M. Sze, Physics of semiconductor devices (1981) John Wiley & Sons.
21. S.P. Tobin, S.M. Vernon, C. Bajgar, V.E. Haven, L.M. Geoffroy, M.M. Sanfacon, D. Lillington, R. Hart, K. Emery, R. Matson, High efficiency GaAs/Ge monolithic tandem solar cells, Proceedings of the 20<sup>th</sup> IEEE Photovoltaic Specialists Conference, (1988) 405.
22. D. Friedman, J. Olson. Analysis of Ge junctions for GaInP/GaAs/Ge three-junction solar cells, Progress in Photovoltaics: Research and Applications **9** (2001) 179.
23. M. Bosi, G. Attolini, C. Ferrari, C. Frigeri, J. Rimada Herrera, E. Gombia E., C. Pelosi, R. Peng, MOVPE growth of homoepitaxial germanium, Journal of Crystal Growth **310** (2008) 3282.